Detection of climate forcing using emission spectra

Richard Goody[1], Robert Haskins, Wedad Abdou, and Luke Chen.
Jet l'repulsion laboratory, California Institute of Technology

March 5, 1995

Abstract

We discuss the use of thermal emission spectra recorded by satellites to construct climate indices that can detect the evolution of a specific climate forcing in a time series. The two important issues arc selectivity against climate forcings other than one that is sought, and sensitivity to the required forcing. We show that indices with selectivity can be found, and that their sensitivity can be high.

1 Introduction

In our present state of knowledge we cannot objectively assess the probable success of a climate projection over a period of 25 to 50 years. The most promising approach to this problem appears to be the application of signal processing techniques to the analysis of climate time series (Hasselmann, 1979, 1994; North *et al*, 1994; North and Kim, 1994; Barnett, 1986; Barnett and Hasselman, 1979; Barnett and Schlesinger, 1987). If a climate forcing can be detected at small signal levels, some confidence may be placed in further projections.

At the basis of such techniques is the comparison between an observed atmospheric state, and what might have been in the absence of a climate forcing. However, we do not know all of the factors involved in the fictional, unforced state, and we cannot predict it. Unless the signal is so large as to leave no doubt as to its presence, the only solution to this dilemma appears to be for the signal of the climate forcing under investigation to be characteristically different from all others. This may not always be possible. For example, the effects upon the climate state of changes in $C0_2$ and N_20 are almost identical. Nevertheless, there arc signals that can discriminate between less similar forcings.

[1] Corresponding author. Mailing address: P.O.Box 430, Falmouth, MA 02541-0430, USA.

One example of a discriminating signal has been discussed by Charlock (1984) and by Kiehl (1983, 1985, 1986). A single spectrum of thermal radiation emitted to space is defined by $\sim$ 10 independent variables. As Kiehl (1986) points out, this gives scope for discriminating between different modes of forcing. There is an additional feature of this signal that has not been emphasized. In climate studies, the first law of thermodynamics acts principally to determine the temperature of the mean emission layer. Given the height of this layer, and the propensity of dynamical factors to produce a fixed temperature lapse rate in the troposphere, this temperature defines the climate state of the lower atmosphere. 'l'his cannot be said about the ground temperature (the most frequently-used climate index), which is separated from the bulk of the atmosphere by a variable boundary layer. The character of the radiation escaping to space has unique significance for understanding the climate.

Atmospheric variables may be recovered by standard inversion techniques from emission spectra with spectral resolutions of 1 to 10 cm^{-1}. This defines the spectral resolution required for discriminating signals. It is quite easy to attain. Such data have been available since the early 1970's and arc a planned part of the EOS missions.

The AIRS spectrometer, scheduled to fly on the second EOS mission, has a spectral range of 650 to 3000 cm^{-1} and a resolving power of 1200 (Aumann and Pagano, 1994). The instrumental noise for AIRS is much less than the observational noise. IRIS was a remarkable fourier transform spectrometer that was flown in the early 1970's on Nimbus 3 and 4 by Hanel and his collaborators. The spectral range of IRIS was 400 to 1600 cm^{-1} and the spectral resolution was 2.8 cm^{-1} (Kunde *et al*, 1974). The system noise is far less than the observational noise. Approximately 9 months' data arc available from Nimbus 4. Both AIRS and IRIS are calibrated against black bodies, and they could be compared with a time separation of 25 years or more, after allowance has been made for the differences in spectral resolution.

IRIS was an instrument ahead of its time. A dvances in detector technology now permit better spectral resolution and a much larger spectral range. Such instruments can now be carried on very small satellites and on unmanned airplanes. To give substance to our discussion we shall consider the possibilities of a continuous series of IRIS measurements, with uncertainties based on the Nimbus 4 data.

The "detection problem" is one of finding an acceptable signal-to-noise ratio: the signal should (if our theories arc correct) correspond to a prediction, *eg* the predicted effect of doubling atmospheric carbon dioxide; while the noise comes from unpredicted, natural events, the spectrum of which is known to extend from hours to decades and longer. Ideally, both signal and noise should be taken from observation, but wc cannot do this because forced climate signals nave not yet been detected, and because the IRIS data extend over only 9 months, so that the spectrum of noise available to us is limited to shorter periods.

We proceeded as follows. We may take the signal from a climate model,

in this case from a radiative-convective model. The noise is treated differently depending upon whether we have data upon it or not. From the IRIS data we obtain "weather" noise with *some* other short-period components. We handle the signal in such a way as to obtain high signal-to-noise ratios against this noise component. We may refer to this as optimizing *sensitivity*.

The atmosphere reaches a steady state with its boundary conditions in about one month. 'Thus, as far as the atmosphere is concerned, noise with periods much longer than a month may be regarded as an unknown forcing, the effects of which will usually differ from the effect of doubling carbon dioxide. We seek methods of processing the data that discriminate as much as possible against examples of these unknown forcings. This we may call seeking selectivity.

The aim of our investigation was to understand how sensitivity and selectivity may be optimized, and how they trade off against each other. We used the signal from doubling carbon dioxide and three other forcings (from changes in the solar constant, relative humidity, and cloud amount), that we consider to be representative of unknown forcings in general. In subsequent papers we expect to present an analysis of long-period noise based upon actual climate data.

2 Climate forcing

Figure 1 shows the four examples of climate forcing in terms of changes of brightness temperature of the outgoing radiation to which they give rise. The associated air temperature changes are shown in figure 2. In each case the change in surface temperature is +1.63 K. This number arose from the calculation for doubled CO_2, shown in the first panel of figure 1. The other three forcings were adjusted to give the same change of surface temperature, so that this parameter cannot be used to distinguish between these forcings.

Dr. Arthur Hou of Goddard Space Flight Center kindly allowed us to use his radiative-tropical convection model to calculate climate changes. Input parameters to this model are the solar flux, water-vapor and CO_2 concentrations, and cloud amount. Details of the model are given by Lindzen *et al* (1982). Radiances were calculated with MODTRAN (Anderson *et al*, 1993), at a resolution of 1 cm^{-1}, and subsequently convolved with the IRIS slit function. 34 levels at 1-km intervals were used in the calculations. The atmosphere above 34 km is neglected.

The climate forcings are defined as follows:

Doubling CO_2. The carbon dioxide is doubled from 330 to 660 ppmv. Following the approach of Kiehl (1986) we have subtracted from the computed results the change that would occur if the carbon dioxide were to vary without changing the temperature. The rationale for this is that the concentration of carbon dioxide is known from chemical measurements, and its purely optical effects can be removed from observed data. These reduced data are influenced only by the changes that take place in temperature and humidity, and provide an

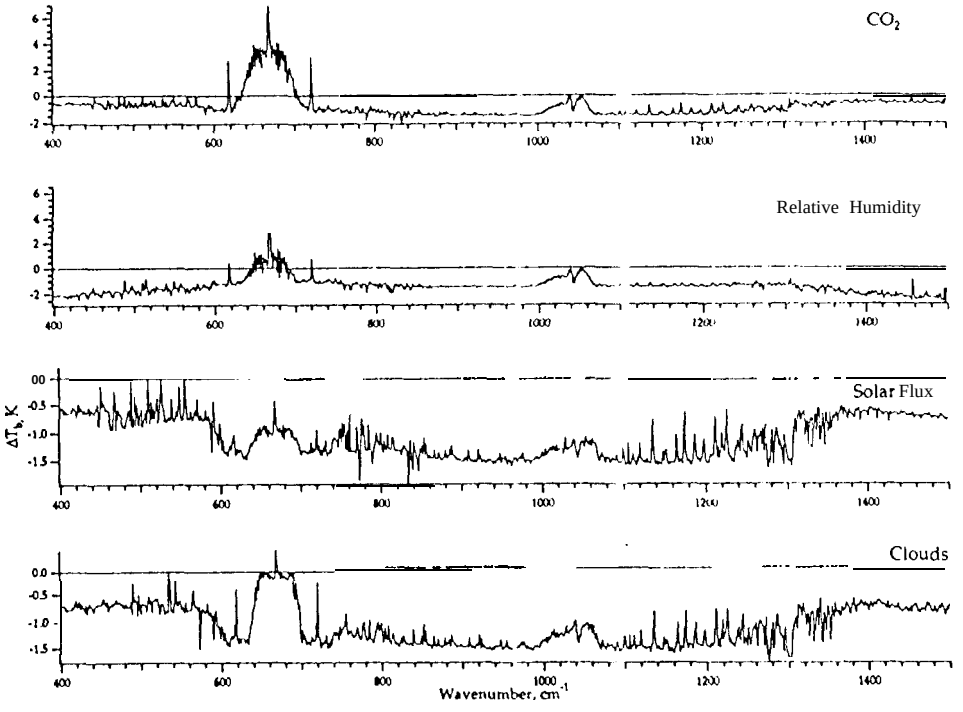

Figure 1: Examples of climate forcing. The four panels show differences in the brightness temperature for four climate forcings, details of which are given in the text. The spectral resolution is the same as for IRIS, 2.8 cm^{-1}.

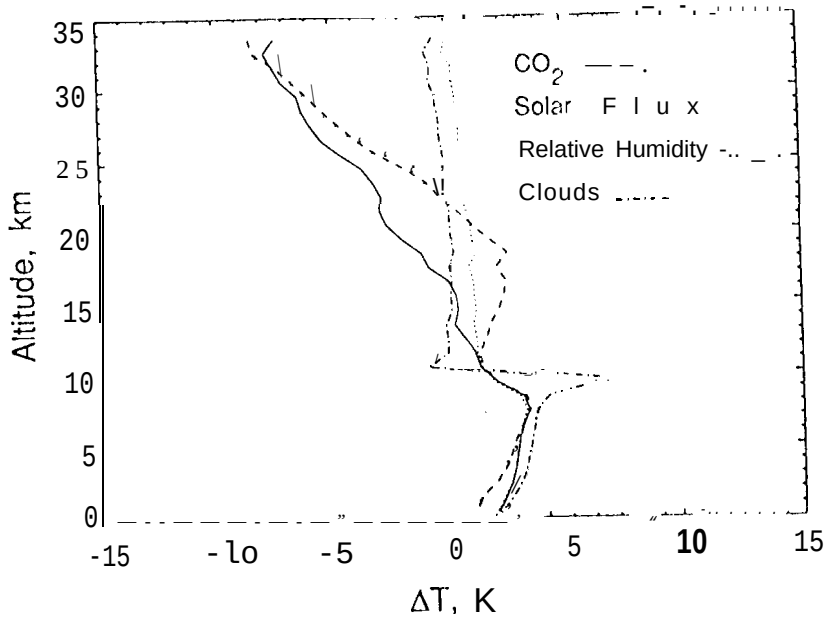

Figure 2: Air temperature changes accompanying climate forcing. The quantity plotted is the change of temperature that goes with the climate changes of figure 1. The change of surface temperature in each case is +1.63 K. 'I'his similarity is by design. The climate model used has a surface boundary layer, so that there is generally a discontinuity of temperature between the surface and the atmosphere.

appropriate for a test of the existence of the predicted climate change.

Relative humidity. The canonical treatment of water vapor in the Hou model is the Manabe-Wetherald climatology for the relative humidity,

$$RH(z) = 0.816\left\{\frac{p(z)}{p(0)} - 0.02\right\}, \; p(z) > 0.02p(0),$$
$$= 0, \; p(z) < 0.02p(0). \tag{1}$$

$p(z)$ is the pressure at altitude, z. Since the relative humidity is given, the model has positive water-vapor feed back, through the temperature. The changed relative humidity that we adopt is defined by,

$$RH(z) = 0.929\left\{\frac{p(z)}{p(0)} - 0.0035\right\}, \; p(z) > 0.0035P(0),$$
$$= 0, \; p(z) < 0.0035p(0). \tag{2}$$

Solar flux. The solar flux was changed from 300 to 305.5 W m^{-2}.

Cloud. MODTRAN has an option to include a model cirrus cloud. The cloud forcing was obtained by including 3.1% cloud cover.

The weather noise is discussed in §5, and spectral data are shown in figure 3. When we compare these data with figure 1 it is immediately apparent that choices of spectral features can greatly influence both sensitivity and selectivity. The maximum signal for carbon dioxide forcing and minimum noise both occur in the center of the 15 μm band, and if sensitivity were the only consideration this would be the optimum wavelength to employ. However, there is no selectivity associated with data from any single wavelength. The question must be examined in greater detail.

3 Selectivity

The observed data are brightness temperatures at times t_i and frequencies ν_k, $T_i(\nu_k)$. We are concerned with differences in the observations at two times t_i and t_j,

$$\Delta_{ij}(\nu_k) = T_i(\nu_k) - T_j(\nu_k). \tag{3}$$

Predicted difference spectra for four different climate changes (figure 1) are designated $\phi(\nu_k), \phi'(\nu_k), \phi''(\nu_k), \phi'''(\nu_k)$. $\phi(\nu_k)$ is the climate change spectrum that we are looking for (*ie* changing CO_2), while we wish to discriminate against the primed spectra.

To do so we weight $\Delta_{ij}(\nu_k)$ with the spectrum $\phi(\nu_k)$. This can be done in a variety of ways: we have explored two using the indices,

$$\tilde{\Delta}_{ij} = \frac{\sum_k \Delta_{ij}(\nu_k)\phi(\nu_k)}{[\sum_k \phi^2(\nu_k) \sum_k 1]^{\frac{1}{2}}}, \tag{4}$$

and,

$$\hat{\Delta}'_{ij} = \frac{\sum_k \{\Delta_{ij}(\nu_k) - \Delta_{ij}\}\{\phi(\nu_k) - \phi\}}{[\sum_k \{\phi(\nu_k) - \phi\}^2 \sum_k 1]^{1/2}}. \tag{5}$$

In equation (5) A_{ij} and ϕ are both averages over the ν_k. Both (4) and (5) are independent of the amplitudes of ϕ_k and of the order of k. The sum over k may be over any spectral region, or over a series of discrete frequencies, provided only that they are contained within the IRIS data. We have investigated five spectral regions, and we report upon four. There is a great deal of room here for selection of optimum climate indices.

What governed our choice of indices as defined in equations (4) and (5)? In the final analysis it is the selectivity and sensitivity that will count, regardless of the reasons for the choice. (4) was chosen because it weights the CO_2 forcing. (5) was chosen in case the selectivity should be adversely affected by mean spectral shifts, that may be common to other forms of forcing.

10 investigate selectivity we substitute first ϕ and then ϕ' in place of A_{ij} in equations (4) and (5) and take ratios. We further normalize the root- mean-square amplitudes of the theoretical spectra to be the same. The absolute values of the ratios then vary over the range O to 1: 1 represents no discrimination in favor of CO_2 forcing, while O represents complete discrimination. The two ratios are:

$$R = \frac{\sum_k \phi'(\nu_k)\phi(\nu_k)}{[\sum_k \phi^2(\nu_k)\sum_k \phi'^2(\nu_k)]^{\frac{1}{2}}}; \tag{6}$$

and,

$$R' = \frac{\sum_k \{\phi(\nu_k) - \phi\}\{\phi'(\nu_k) - \phi'\}}{[\sum_k \{\phi(\nu_k) - \phi\}^2 \sum_k \{\phi'(\nu_k) - \phi'\}]^{1/2}}. \tag{7}$$

Equation (7) is the conventional correlation coefficient between ϕ and ϕ'.

Tables 1 and 2 show calculations from (6) and (7) when ϕ' is change of humidity, change of solar constant, or change of cloud amount. These calculations are for four spectral ranges. The first row includes all IRIS data. The second and third rows split this range at the high-frequency wing of the 15 μm CO_2 band. The third row is dominated by the water-vapor continu urn, the behavior of which depends chiefly on the common change in ground temperature. The fourth row is essentially limited to the 15 μm band.

In tables 1 and 2 we should note the signs. A positive sign implies that the forcing can reinforce $C0_2$, while a negative sign implies that the unwanted forcing may counteract it; either confuses conclusions about cause and effect. Only small absolute values of (6) and (7) are helpful. In this respect the most important feature of tables 1 and 2 is that a small absolute value exists for each forcing under at least one circumstance; but no single circumstance gives good selectivity for all three forcings. An added consideration is that, when selectivity is good, the signal-to-noise ratio, and hence the sensitivity, may be

Table 1: Selectivity of climate indices. The table compares values from equation (6) for four spectral ranges. The final column is the square of a signal-to-noise ratio that will be discussed in §5.

spectral region, cm^{-1}	R from equation (6) humidity	solar rad.	cloud	$(S/N)^2$
400.5-1486.5	+.774	+.659	+.771	13.1
400.5-700.0	+.552	−.131	+.290	4.85
700.0-1450.0	+.915	+.970	+.974	9.05
600.0-740.0	+.614	−.299	+.157	7.16

Table 2: Selectivity of climate indices. As for table 1, but using equation (7).

spectral region, cm^{-1}	R' from equation (7) humidity	solar rad.	cloud	$(S/N)^2$
400.5-1486.5	+.686	+.379	+.773	0.94
400.5-700.0	+.907	−.195	+.752	4.40
700.0-1450.0	+.100	+.722	+.780	0.97
600.0-740.0	+.887	+.879	+.995	16.59

too small to be useful. An example is the relative humidity forcing in table 2 for 700-1450 cm^{-1}.

A feature of table 1 is the lack of selectivity for the index $\hat{\Delta}_{ij}$ in the spectral range 700.0 -1450.0 cm-l. This range is dominated by the surface and near-surface temperature, a single parameter, for which selectivity is not possible. It does not give a notably high signal-to-noise ratio. This comment has significance with respect to the conventional use of series of ground temperature measurements to detect climate ch angc. The selectivity for this spectral region is improved by the use of the index (5), which eliminates the effect of a uniform shift in the emission temperature (an important contribution from the water-vapor window region), see table 2, but at t he expense of sensitivity.

In the following sections we confine our attention to the spectral range 600.0-740.0 cm^{-1}, for the reasons that table 1 shows some selectivity, with above average signal-to-noise ratio, while table 2 shows exceptional signal-to-noise ratio. The choice of climate index and spectral range will dependon the question that an investigator wishes to ask. In this paper we seek only to demonstrate that useful choices may be made.

4 Sensitivity

A_{ij} (and similarly for $\hat{\Delta}'_{ij}$) contains a term $\tilde{\Delta}^S_{ij}$, which is the signal that is sought. The $C0_2$ signal should, for small changes, be proportional to $\rho_{ij} = \rho_i - \rho_j$, where ρ is the density of $C0_2$. For the calculations shown in the first panel of figure 1, $\rho_{ij} = \rho_0$, where ρ_0 is the current density of $C0_2$, *ie* the change concerns doubling the density from ρ_0 to $2\rho_0$. *The* important question is to what degree the brightness temperature is sensitive to the density of CO_2. To assess this, we evaluate the correlation coefficient between $\hat{A}_{ij}$ and ρ_{ij},

$$r = \frac{\sum_{ij} \tilde{\Delta}_{ij} \rho_{ij}}{\left[\sum_{ij} \tilde{\Delta}^2_{ij} \sum_{ij} (\rho^2_{ij} - \rho^2)\right]^{\frac{1}{2}}}, \tag{8}$$

where $p \frac{\sum_{ij} \rho_{ij}}{\sum_{ij} 1}$ is the mean value of ρ_{ij} over the period of observation. The mean value of $\tilde{\Delta}_{ij}$ is, by virtue of the definition (3), identically zero.

The significance of the correlation may be tested with the t-distribution. For 90% significance,

$$r^2 \approx \frac{4}{D - 2} \approx \frac{4}{D}, \tag{9}$$

where D is the number of independent degrees of freedom. For 70% significance,

$$r^2 \approx \frac{2}{D}. \tag{lo}$$

Later we shall assume that there are α independent climate observations in one year, so that,

$$D = \alpha y, \tag{11}$$

where y is the number of years over which the observations extend.

The slope of the regression,

$$b = r \left[\frac{\sum_{ij} (\hat{\Delta}_{ij}^2 - \quad ^2)}{\sum_{ij} (\rho_{ij}^2 \quad \rho^2)} \right]^{\frac{1}{2}} \quad \text{«} \tag{12}$$

is the rate of change of brightness temperature with CO_2 density change, the quantity that theories can predict.

Next, we assume that the observations can be unambiguously' separated into climate signal and climate noise,

$$\hat{\Delta}_{ij} = \tilde{\Delta}_{ij}^S + \tilde{\Delta}_{ij}^N, \tag{13}$$

where $\tilde{\Delta}_{ij}^S$ is the signal, and $\tilde{\Delta}_{ij}^N$ is the noise,

$$\sum_{ij} \tilde{\Delta}_{ij}^N = 0. \tag{14}$$

This separation is difficult to justify objectively. However, the same assumption is made by all other investigators known to us, and appears to be unavoidable.

The signal is obtained by substituting,

$$\Delta_{ij}(\nu_k) = \frac{\rho_{ij}}{\rho_0} \phi(\nu_k), \tag{15}$$

in equation (4), to give,

$$\tilde{\Delta}_{ij}^S = \frac{\rho_{ij}}{\rho_0} \left\{ \frac{\sum_k \phi^2(\nu_k)}{\sum_k 1} \right\}^{1/2}. \tag{16}$$

Use of the alternative climate index, equation (5), is accomplished by replacing $\phi(\nu_k)$ by $\phi(\nu_k)$ -4.

The correlation coefficient, (8), can now be written,

$$r^2 = \frac{S^2}{\bar{N}} \cdot \frac{\sum_{ij} \frac{\rho_{ij}^2 - \rho^2}{\rho_0^2}}{\sum_{ij} 1} \cdot) \tag{17}$$

where the square of the "signal" is,

$$S^2 = \frac{\sum_k \phi^2(\nu_k)}{\sum_k 1}, \tag{18}$$

and tbc square of the "noise" is,

$$N^2 = \frac{\sum_{ij} (\tilde{\Delta}_{ij}^N)^2}{\sum_{ij} 1}. \tag{19}$$

We may evaluate the term $\sum_{ij} \frac{\rho_{ij}^2 - \rho^2}{\rho_0^2} \Big/ \sum_{ij}$ for the special case of continuing, frequent observations. If we observe for y years with an increase ρ_1 per year, the maximum ρ_{ij} is $y\rho_1$. The sum involves all ρ_{ij} less than this amount. If the number of samples is large and if they are evenly distributed over y years, we may evaluate the sum as a double integral,

$$\frac{\sum_{ij} \frac{\rho_{ij}^2 - \rho^2}{\rho_0^2}}{\sum_{ij} 1} = \frac{1}{18} y^2 \left(\frac{\rho_1}{\rho_0} \right)^2. \tag{20}$$

The current value for the ratio $\frac{\rho_1}{\rho_0}$ is 5×10^{-3}.

5 Noise

The signal, equation (18), is unambiguous. The difficulty in assessing sensitivity lies in calculating the noise term, (19), and deciding upon the number of independent degrees of freedom. In fact, climate noise is a function of the period of averaging or of observation. It must be treated by tirnc-series analysis, and a simple correlation coefficient is an inappropriate measure of the emergence of a signal. We cannot, however, perform a more sophisticated analysis with the data available.

We use equation (19) but with $\tilde{\Delta}_{ij}$ in place of $\tilde{\Delta}_{ij}^N$. Over the period with which we shall be concerned there is little difference between these two quantities because the noise dominates the signal. This procedure slightly overestimates the noise.

$\tilde{\Delta}_{ij}$ is calculated from equations (4) or (5) using 1 l-day means of IRIS data. We assume that each 1 l-day mean is an independent data set. On this basis wc estimate that there are 30 independent data sets in each year. This procedure probably underestimates the noise, and overestimates the number of degrees of freedom; our conclusions probably err on the side of optimism.

The IRIS data were partitioned into latitude zones, as indicated in table 3, and selected for clear skies on the basis that the emission temperature in the water-vapor window is within 10 K of the sea-surface climatology of Reynolds (1982). The calculations in table 3 are for clear skies, and the spectral range 600.0 to 740.0 cm-l. 'l'he data come from a variety of locations in each geographical region and cent ain an avoidable "geographic" noise component; on this account our noise estimates are larger than they need to be.

From the data in table 3 we conclude that the tropics give better signal-to-noise ratios than other latitudes. Since there is a very large amount of tropical

'1'able 3: Spectral noise from IRIS data. The data arc for clear skies and for 600.0 to 740.0 cm^{-1}. Compare these results to the square of the signal, 4.78 K^2 for index (4), and 3.88 K^2 for index (5).

zone	latitudes	longitudes	N^2, K^2 equ.(4)	equ.(5)
equatorial	-10 to +10	--180 to +180	0.67	0.23
warm pool	--10 to +10	+120 to -1150	0.56	0.38
N mid-latitudes	+30 to +50	--180 to +180	4.70	2.15
S mid-latitudes	–30 to –50	–180 to +180	5.00	1.93
N Pacific	+45 to +60	–180 to -135	13.4	5.19

IRIS data, there is little to be gained by including extra-tropical latitudes. Table 3 also indicates a slight advantage of index (5) over (4).

Important insights into the character of the climate indices can be obtained from the spectrum of emission temperature variance, sec figure 3. These calculations arc for l-day means. For n-day means the standard deviation should be smaller by a factor $\sim\sqrt{11}$. l'he data illustrate two points, the first being the superiority of tropical, clear-sky data. The second is the complex nature of the spectral character of our climate indices. As was pointed out earlier, figure 1 is the signal, and figure 3 is the noise, and the investigator is free to choose any frequencies. Comparison between these two figure clearly illustrates the wide range of choices that are available for the climate indices.

6 Discussion

From (9), (12), (17), and (20) the number of years required for detection with 90% significance is given from,

$$y^3 \approx \frac{72}{\alpha} \left(\frac{\rho_0}{\rho_1}\right)^2 \left(\frac{N}{S}\right)^2 . \tag{21}$$

For 70% significance the numerical factor should be halved. Table 4 shows the number of years to detection of $C0_2$ forcing, based on equations (21) and (4), for clear skies in the tropics, and for the spectral range 600.0 to 740.0 cm^{-1}. Calculations have been made for 70% and 90% certainty, and for both the $C0_2$ forcing that we have discussed, and for twice this forcing. A ground temperature change of 3.26 K is closer to the median of calculations made with other climate models. For a ground-temperature change for CO_2 doubling of 3.26 K, and

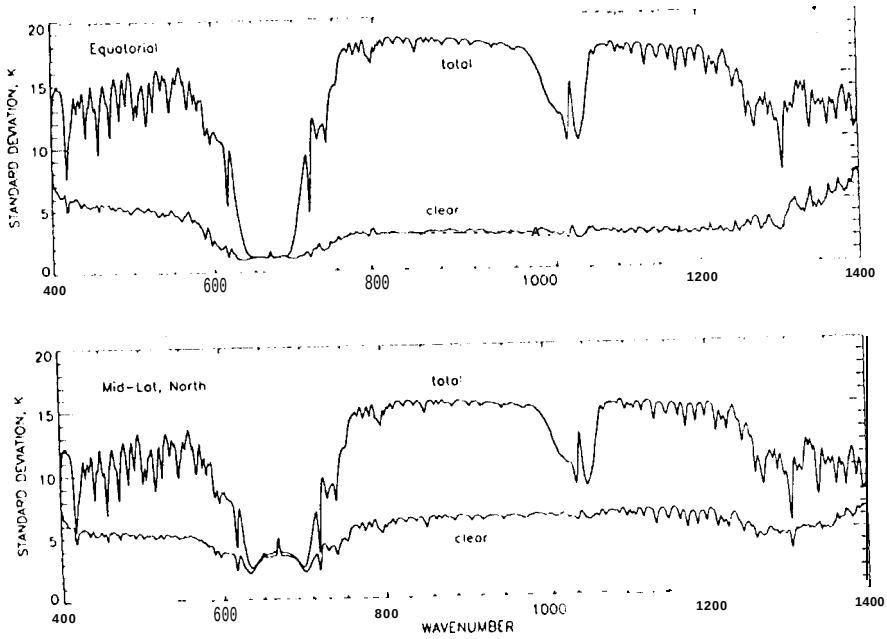

Figure 3: Spectra of the standard deviation of the emission temperature. Daily means are used. For clear skies alone and for all data together, for the equatorial and N mid-latitude zones.

Table 4: Years to detection. Calculations are for index (4), the tropical zone, clear skies, and the spectral range 600.0 -740.0 cm^{-1}. We assume α = 30, and $\frac{\rho_1}{\rho_0} = 5.7 \times 10^{-3}$. For the climate index (5), columns 4, 5, and 6 should be divided by 1.32.

case	significance	ΔT_g(2 x CO_2), K	years	%rise	ΔT_g(detected), K.
1	90%	1.63	21.8	12.4	0.20
2	90%	3.26	13.7	7.8	0.25
3	70%	1.63	17.2	9.8	0.16
4	70%	3.26	10.9	6.2	0.20

for 70% certainty, the calculation suggests detection after 10.9 years when CO_2 concentrations have risen by 6.2%, and the surface temperature has risen by 0.2 K. For the climate index (5), these figures should all be reduced by the factor 1.32.

These numbers are principally of qualitative significance. The time to detection is encouragingly short, but a more satisfactory time-series analysis should be made. Such analysis requires knowledge of noise on time scales longer than the period of the IRIS data. Data may be obtained from existing archives of climate data or from model simulations, and the outgoing spectrum can be constructed by MO DTRAN. We intend to perform this analysis in the near future.

Our purpose in this paper has been to illustrate the possibility of developing climate indices that may be more sensitive than conventional indices, and which may, at the same time, be selective towards one particular climate forcing. There is a wide choice of possible indices. There is nothing unique about the indices in equations (4) and (5), and we have not covered all of the possibilities associated with the spectral summation.

Finally, we may relate this discussion to current attempts to use the geographical distribution of signal and noise to optimize the detection of a forced signal in a climate time series. Hasselman and Barnett (1979) introduced the basic formalism by representing the forced climate signal in terms of Empirical Orthogonal Functions (EOF's), and using a null hypothesis to test for a forced climate response in the projection of the data set on the EOF's. Barnett (1986) extended this idea to multiple, geographically-based climate indicators, which be called "fingerprints", using pattern correlation techniques, again exploiting the basic EOF formalism. Recently both Hasselman (1995) and North *et al* (1995) have extended Barnett's work by prefiltering the input data stream to enhance the signal-to-noise ratio. In essence, their work rotates the projections into directions least affected by climate noise.

The work of these authors could be extended to make usc of our spectral indices, if they were evaluated by geographical region. in addition, North's formalism lends itself to evaluating EOF's in the frequency domain, from the data in figure 3. We have made calculations based on EOF expansions of tbc IRIS noise data in the frequency domain. The results of our study show approximately 50% enhancement of the signal in tile highly variable water-vapor regions of the infrared spectrum, but little enhancement in the more important 15 pm carbon dioxide band.

7 Acknowledgements

Wc wish to acknowledge the help of Sheppard Clough of Atmospheric and Environmental Research Inc. in gaining access to the IRIS data. The research described in this paper was carried out at the Jet Propulsion laboratory, California Institute of Technology, under contract with the National Aeronautics and Space Administration.

8 References

Aumann, 11.11., and Pagano, R. J., 1994: "Atmospheric infrared sounder on the Earth Observing System", *Optical Engineering* 33(3), 776-784.

Anderson, G.I'., *et al,* 1993: "MODTRAN2: Suitability for remote sensing", *Proc. Sot. Photo-Optical Inst. Eng.* **1968**, 514-525.

Barnett, 'J'. P., 1986: "Detection of changes in the global tropospheric temperature field induced by greenhouse gases", 3. *Geophys. Res.* 91, 6659-6667.

Barnett, T. P., and Hasselman, K., 1979: "Techniques of linear prediction with application to oceanic and atmospheric. fields in the tropical Pacific", *Rev. Geophys. Space Phys.* 17, 949-968.

Barnett, T., and Schlesinger, M., 1987: "Detecting changes in global climate induced by greenhouse gases", *J. Geophys. Res.* 92, 14,772-14,780.

Charlock, T. P., 1984: "CO_2 induced climatic change and spectral variations *in* the outgoing terrestrial infrared radiation", *Tellus* **36B**, *139-148.*

Hasselman, K., 1979: '(On the signal to noise problem in atmospheric response studies", *Meteorology of Tropical Oceans.* London: Royal Meteorological Society, 251-259.

Hasselmann, K., 1994: '(optimum fingerprints for the detection of time-dependent climate change", submitted to *J. Climate.*

Kiehl, J .P., 1983: "Satellite detection of effects duc to increased atmospheric carbon dioxide", Science 222, 504-506.

Kiehl. J.} '., 1985: "Searching for the radiative signal of increasing carbon dioxide and other trace gases", *Effects of increasing carbon* dioxide, M.C.McCracken and F. M. Luther, Eds., DOE/ER-0235, 15-27.

Kiehl, J .1'., 1986: "Changes in the radiative balance of the atmosphere due to increase in $C0_2$ and trace gases", *Adv. Space Res.* **6,** No.1O, 55-60.

Kunde, V. G., Conrath, B.J., Hanel, R. A., McGuire, W. C., Prabhakara, C., and Salomonson, V. V., 1974: "The Nimbus 4 spectroscopy experiment 2. Comparison of observed and theoretical radiances for 325-1450 Cm- ^{1}", *J. Geophs. Res.* 79, 777-784.

North, G. R., Kim, K-Y, Shen, S. S.1'., and Hardin, J. W., 1995: "Detection of forced climate signals Part 1: Filter theory", submitted to *J. Climate.*

North, G. R., and Kim, K-Y, 1995: "Detection of forced climate signals Part II: Simulation results", submitted to *J. Climate.*

Reynolds, R, 1982: "A monthly averaged climatology of surface temperature", *NOAA Technical Report,* NWS 31.